

# Carleman estimates and the contraction principle for an inverse source problem for nonlinear hyperbolic equations

Loc H. Nguyen\*

Michael V. Klibanov†

## Abstract

The main aim of this paper is to solve an inverse source problem for a general nonlinear hyperbolic equation. Combining the quasi-reversibility method and a suitable Carleman weight function, we define a map of which fixed point is the solution to the inverse problem. To find this fixed point, we define a recursive sequence with an arbitrary initial term by the same manner as in the classical proof of the contraction principle. Applying a Carleman estimate, we show that the sequence above converges to the desired solution with the exponential rate. Therefore, our new method can be considered as an analog of the contraction principle. We rigorously study the stability of our method with respect to noise. Numerical examples are presented.

*Key words:* numerical methods; Carleman estimate; contraction principle; globally convergent numerical method, nonlinear hyperbolic equations.

*AMS subject classification:* 35R30; 65M32.

## 1 Introduction

Let  $d \geq 2$  be the spatial dimension. Let  $F : \mathbb{R}^d \times [0, \infty) \times \mathbb{R} \times \mathbb{R} \times \mathbb{R}^d \rightarrow \mathbb{R}$  be a function in the class  $C^1$ . For  $u \in C^2(\mathbb{R}^d \times (0, \infty))$ , define the operator  $\mathcal{F}$  as

$$\mathcal{F}u(\mathbf{x}, t) = F(\mathbf{x}, t, u, u_t, \nabla u) \quad \text{for all } (\mathbf{x}, t) \in \mathbb{R}^d \times (0, \infty).$$

Let  $c : \mathbb{R}^d \rightarrow [1, \bar{c}]$ , for some given finite number  $\bar{c}$ , be a function in the class  $C^2(\mathbb{R}^d)$ . Consider the following initial value problem

$$\begin{cases} c(\mathbf{x})u_{tt}(\mathbf{x}, t) = \Delta u(\mathbf{x}, t) + \mathcal{F}u(\mathbf{x}, t) & (\mathbf{x}, t) \in \mathbb{R}^d \times (0, \infty), \\ u_t(\mathbf{x}, 0) = 0 & \mathbf{x} \in \mathbb{R}^d, \\ u(\mathbf{x}, 0) = \mathbf{p}(\mathbf{x}) & \mathbf{x} \in \mathbb{R}^d \end{cases} \quad (1.1)$$

where  $\mathbf{p}$  is the initial source function. Let  $\Omega$  be an open and bounded domain in  $\mathbb{R}^d$  with smooth boundary  $\partial\Omega$ . Let  $T$  be a positive number. Define  $\Omega_T = \Omega \times [0, T]$  and  $\Gamma_T = \partial\Omega \times [0, T]$ . The reader can find the conditions on  $\mathbf{p}$ ,  $c$  and  $F$  that guarantee the existence, uniqueness and regularity results for (1.1) in many textbooks about PDEs, see e.g. [8, 12]. Studying the these properties is of (1.1) is out of the scope of this paper. We consider them as assumptions. The main aim of this paper is to solve the following inverse problem:

\*Department of Mathematics and Statistics, University of North Carolina at Charlotte, Charlotte, NC, 28223, USA, [loc.nguyen@uncc.edu](mailto:loc.nguyen@uncc.edu) (corresponding author).

†Department of Mathematics and Statistics, University of North Carolina at Charlotte, Charlotte, NC, 28223, USA, [mklibanv@uncc.edu](mailto:mklibanv@uncc.edu).

**Problem 1.1** (An inverse source problem for nonlinear hyperbolic equations). *Determine the source function  $\mathbf{p}(\mathbf{x})$ ,  $\mathbf{x} \in \Omega$ , from the lateral Cauchy data*

$$f(\mathbf{x}, t) = u(\mathbf{x}, t) \quad \text{and} \quad g(\mathbf{x}, t) = \partial_\nu u(\mathbf{x}, t) \quad (1.2)$$

for all  $(\mathbf{x}, t) \in \Gamma_T$ .

Problem 1.1 can be considered as the nonlinear version of the important problem arising from bio-medical imaging, called thermo/photo-acoustics tomography. The experiment leading to this problem is as follows, see [35, 36, 46]. One sends non-ionizing laser pulses or microwave to a biological tissue under inspection (for instance, woman's breast in mamography). A part of the energy will be absorbed and converted into heat, causing a thermal expansion and a subsequence ultrasonic wave propagating in space. The ultrasonic pressures on a surface around the tissue are measured. Finding some initial information of the pressures from these measurements yields the structure inside this tissue. The current techniques to solve the problem of thermo/photo-acoustics tomography are only for linear hyperbolic equation. We list here some widely used methods. In the case when the waves propagate in the free space, one can find explicit reconstruction formulas in [11, 13, 43, 45], the time reversal method [20, 17, 18, 49, 50], the quasi-reversibility method [10, 41] and the iterative methods [19, 47, 48]. The publications above study thermo/photo-acoustics tomography for simple models for non-damping and isotropic media. The reader can find publications about thermo/photo-acoustics tomography for more complicated model involving a damping term or attenuation term [3, 2, 14, 1, 9, 16, 33, 34, 42]. Up to the author's knowledge, this inverse source problem when the governing equation is general and nonlinear like (1.1) is not solved yet.

Natural approaches to solve nonlinear inverse problem are based on optimization. These approaches are local in the sense that they only deliver solutions if good initial guesses of the solutions are given. The local convergence does not always hold unless some additional conditions are imposed. We refer the reader to [15] for a condition that guarantees the local convergence of the optimization method using Landweber iteration. The question how to compute the solutions to nonlinear problems without requesting a good initial guess is very interesting, challenging and significant in the scientific community. There is a general framework to globally solve nonlinear inverse problem, called convexification. The main idea of the convexification method is to employ some suitable Carleman weight functions to convexify the mismatch functional. The convexified phenomenon is rigorously proved by employing the well-known Carleman estimates. Several versions of the convexification method [4, 23, 24, 25, 27, 29, 31, 30, 32, 40] have been developed since it was first introduced in [28]. Especially, the convexification was successfully tested with experimental data in [21, 22, 30]. Although effective, the convexification method has a drawback. It is time consuming. We therefore propose a new method based on the fixed-point iteration, the contraction principle and a suitable Carleman estimate to globally solve nonlinear inverse problems. This new method is considered as the second generation of globally convergent numerical methods to solve nonlinear inverse problems while the convexification method is the first one.

Our approach to solve Problem 1.1 is to reformulate it to be of the form  $\Phi(x) = x$  for some operator  $\Phi$ . The general framework to find the fixed point of  $\Phi$  in this paper is to construct a sequence by the same the sequence defined in the classical proof of the contraction principle. Take any initial solution to the nonlinear inverse problem, denoted by  $x_0$  and then recursively define  $x_n = \Phi(x_{n-1})$  for  $n > 0$ . In general, the convergence of  $\{x_n\}_{n \geq 0}$  to the fixed point of  $\Phi$  is not guaranteed. However, we discovered recently in [39], see also [5, 6], that if we include some suitable Carleman weight function in the definition of  $\Phi$  then the convergence holds true. In the current

paper, we define  $\Phi$  by including the Carleman weight function in [26, Lemma 6.1] and [7, Theorem 1.10.2] into the classical quasi-reversibility method, which was first introduced in [37]. The proof of the contractional behavior of  $\Phi$  relies on the Carleman estimate in [26, Lemma 6.1] and [7, Theorem 1.10.2]. The main theorems in this paper confirm that the recursive sequence above converges to the true solution. The stability with respect to the noise contained in the given data is of the Hölder type.

The paper is organized as follows. In Section 2, we introduce our iteration. In Section 3, we prove the convergence of the sequence generated in Section 2. In Section 4, we present some numerical tests. Section 5 is for concluding remarks.

## 2 An iterative method to solve Problem 1.1

Problem 1.1 can be reduced to the problem of computing a function  $u = u(\mathbf{x}, t)$  defined on  $\Omega \times [0, T]$  satisfying the following problem involving a nonlinear hyperbolic equation, the lateral Cauchy data and an initial condition

$$\begin{cases} c(\mathbf{x})u_{tt}(\mathbf{x}, t) = \Delta u(\mathbf{x}, t) + \mathcal{F}u(\mathbf{x}, t) & (\mathbf{x}, t) \in \Omega_T, \\ u(\mathbf{x}, t) = f(\mathbf{x}, t) & (\mathbf{x}, t) \in \Gamma_T, \\ \partial_\nu u(\mathbf{x}, t) = g(\mathbf{x}, t) & (\mathbf{x}, t) \in \Gamma_T, \\ u_t(\mathbf{x}, 0) = 0 & \mathbf{x} \in \Omega. \end{cases} \quad (2.1)$$

In the case of success, one can set  $\mathbf{p}(\mathbf{x}) = u(\mathbf{x}, 0)$  for all  $\mathbf{x} \in \Omega$  as the computed solution to Problem 1.1. Due to the presence of the nonlinearity  $\mathcal{F}$ , numerically solving (2.1) is extremely challenging. Conventional methods to do so are based on optimization. That means, one minimizes some mismatch functionals, for e.g.,

$$u \mapsto \int_{\Omega_T} \left| c(\mathbf{x})u_{tt}(\mathbf{x}, t) - \Delta u(\mathbf{x}, t) - \mathcal{F}u(\mathbf{x}, t) \right|^2 + \text{a regularization term}$$

subject to the boundary and initial constraints in the last three lines of (2.1). The computed solution to (2.1) is set as the obtained minimizer. However, due to the nonlinearity  $\mathcal{F}$ , such a functional is not convex. It might have multiple minima and ravines. Therefore, the success of the methods based on optimization depends on the good initial guess. In reality, good initial guesses are not always available. Motivated by this challenge, we propose to construct a fixed-point like iterative sequence based on the quasi-reversibility method and a Carleman estimate in [26, Lemma 6.1] and [7, Theorem 1.10.2]. The convergence of this sequence to compute solution to (2.1) will be proved by the contraction principle and a Carleman estimate. Our Carleman-based iterative algorithm to numerically solve (2.1) is as follows.

Let  $\mathbf{x}_0$  be a point in  $\mathbb{R}^d \setminus \bar{\Omega}$ . For  $\lambda > 0$  and  $\eta > 0$ , define the Carleman weight function

$$W_{\lambda, \eta}(\mathbf{x}, t) = e^{\lambda(|\mathbf{x} - \mathbf{x}_0|^2 - \eta t^2)} \quad \text{for all } (\mathbf{x}, t) \in \Omega_T. \quad (2.2)$$

Let  $p > [(d+1)/2] + 2$  where  $[(d+1)/2]$  is the smallest integer that is greater than or equal to  $(d+1)/2$ . Then,  $H^p(\Omega_T)$  is continuously embedded into  $C^2(\Omega_T)$ . The convergence of our method to solve (2.1) is based on the following Carleman weighted norms.

**Definition 2.1** (Carleman weighted Sobolev norms). *For all  $\lambda \in (1, \infty)$ ,  $\eta \in [0, 1]$  and  $s \in \mathbb{N}$ , we define the norm*

$$\|v\|_{H_{\lambda, \eta}^s(\Omega_T)} = \left[ \sum_{|\alpha|=0}^s \int_{\Omega_T} W_{\lambda, \eta}^2(\mathbf{x}, t) |D_\alpha v|^2 dt d\mathbf{x} \right]^{1/2} \quad \text{for all } v \in H^s(\Omega_T). \quad (2.3)$$

The notation  $D_\alpha$  in (2.3) is understood in the usual sense. That means,  $\alpha = (\alpha_1, \dots, \alpha_d, \alpha_{d+1})$  being a  $d+1$  dimensional vector of nonnegative integers,  $|\alpha| = \sum_{i=1}^{d+1} \alpha_i$  and  $D_\alpha = \frac{\partial^{|\alpha|}}{\partial x_1^{\alpha_1} \dots \partial x_d^{\alpha_d} \partial t^{\alpha_{d+1}}}$ .

Assume that the set of admissible solutions

$$H = \{u \in H^p(\Omega_T) : u_t|_{\Omega \times \{0\}} = 0, u|_{\Gamma_T} = f \text{ and } \partial_\nu u|_{\Gamma_T} = g\}$$

is nonempty. We construct a sequence  $\{u_n\}_{n \geq 0} \subset H$  that converges to the solution to (2.1). Take an arbitrary function  $u_0 \in H$ . Assume by induction that  $u_n$  is known. We set  $u_{n+1} = \Phi(u_n)$  where  $\Phi(u_n)$  is the unique minimizer of  $J_n : H \rightarrow \mathbb{R}$  defined as

$$J_n(v) = \int_0^T \int_\Omega W_{\lambda,\eta}^2(\mathbf{x}, t) |c(\mathbf{x})v_{tt} - \Delta v - \mathcal{F}(u_n)|^2 d\mathbf{x}dt + \epsilon \|v\|_{H_{\lambda,0}^p(\Omega_T)}^2 \quad \text{for all } v \in H. \quad (2.4)$$

See (2.3) for the norm of the regularity term  $\epsilon \|v\|_{H_{\lambda,0}^p(\Omega_T)}^2$ . Due to the compact embedding from  $H^p(\Omega_T)$  to  $H^2(\Omega_T)$ , the functional  $J_n$  is weakly lower semi-continuous. The presence of the regularization term guarantees that  $J_n$  is coercive. Hence,  $J_n$  has a minimizer  $u_{n+1}$  on the close and convex set  $H$  in  $H^p(\Omega_T)$ . The uniqueness of  $u_{n+1}$  is due to the strict convexity of  $J_n$ . An alternative way to obtain the existence and uniqueness of the minimizer is to argue similarly to the proofs of Theorem 2.1 in [4] or Theorem 4.1 in [30]. We will prove that the sequence  $\{u_n\}_{n \geq 0}$  converges to the solution to (2.1). This suggests Algorithm 1 to solve Problem 1.1.

---

**Algorithm 1** A procedure to compute the numerical solution to Problem 1.1

---

- 1: Choose a number  $n_0$  that represents the maximal number of iteration. Choose an arbitrary initial solution  $u_0 \in H$ .
  - 2: **for**  $n = 0$  to  $n_0$  **do**
  - 3:   Minimize the function  $J_n$ , defined in (2.4), on  $H$ .
  - 4:   Set  $u_{n+1}$  as the obtained minimizer.
  - 5: **end for**
  - 6: Set the computed solution to (2.1) as  $u_{\text{comp}} = u_{n_0}$ .
  - 7: Set the computed solution to Problem 1.1 as  $\mathbf{p}_{\text{comp}}(\mathbf{x}) = u_{\text{comp}}(\mathbf{x}, 0)$  for all  $\mathbf{x} \in \Omega$ .
- 

**Remark 2.1.** The presence of the Carleman weight functions  $W_{\lambda,\eta}(\mathbf{x}, t)$  and that of the weight function  $W_{\lambda,0}(\mathbf{x}, t)$  in the regularization term in (2.4) play the key role in proving the convergence of the sequence  $\{u_n\}_{n \geq 0}$  to the true solution to (1.1). See Theorem 3.1 for details.

**Remark 2.2.** One can replace the homogeneous initial condition for  $u_t(\mathbf{x}, 0)$  in (1.1) by the non-homogenous one  $u_t(\mathbf{x}, 0) = \mathbf{q}(\mathbf{x})$  for all  $\mathbf{x} \in \mathbb{R}^d$  for some given function  $\mathbf{q}$ . The analysis leading to the numerical method and the proof for the convergence of the method will be the same.

**Remark 2.3.** Besides Algorithm 1, one can apply the convexification method, first introduced in [28], to globally solve (2.1) and Problem 1.1. In fact, by combining the arguments in [4, 10, 30], one can prove that:

1. for any large ball  $B(M) = \{u \in H^p(\Omega_T) : \|u\|_{H^s(\Omega_T)} < M\}$  of  $H^s(\Omega_T)$  where  $M$  is an arbitrarily large number, the functional

$$u \mapsto \int_{\Omega_T} W_{\lambda,\eta}^2(\mathbf{x}, t) \left| c(\mathbf{x})u_{tt}(\mathbf{x}, t) - \Delta u(\mathbf{x}, t) - \mathcal{F}u(\mathbf{x}, t) \right|^2 + \text{a regularization term}$$

is strictly convex in the large ball of  $H^s(\Omega_T)$  for all  $\lambda$  sufficiently large and  $\eta$  sufficiently small;

2. the unique minimizer of this functional in  $B(M)$  is a good approximation of the desired solution.

In theory, both Algorithm 1 and the convexification method deliver reliable solution to (2.1) without requesting initial guess. It is interesting to verify the efficiency of the convexification method while that of Algorithm 1 is confirmed in this paper. Developing the convexification method for (2.1) and verify it numerically serve as one of our future research topics.

### 3 The convergence theorem

In this section, we employ a Carleman estimate, see [26, Lemma 6.1] and [7, Theorem 1.10.2] to prove the convergence of the sequence  $\{u_n\}_{n \geq 0}$  obtained by Algorithm 1 to the true solution to (2.1).

#### 3.1 The statement of the convergence theorem

Since  $\Omega$  is a bounded domain, it is contained in a large disk  $D = B(R) = \{\mathbf{x} \in \mathbb{R}^d : |\mathbf{x}| < R\}$  for some positive number  $R$ . Before stating the convergence theorems, we recall an important Carleman estimate. For  $\eta > 0$  and  $\varepsilon > 0$ , define

$$D_{\eta, \varepsilon} = \{(\mathbf{x}, t) \in D \times [0, \infty) : |\mathbf{x} - \mathbf{x}_0|^2 - \eta t^2 > \varepsilon\}. \quad (3.1)$$

The following lemma plays a key role in our analysis.

**Lemma 3.1** (Carleman estimate). *Assume that the point  $\mathbf{x}_0$  in the definition of the Carleman weight function in (2.2) is in the set  $D \setminus \overline{\Omega}$  and that the coefficient  $c$  in (1.1) satisfies the condition*

$$\langle \mathbf{x} - \mathbf{x}_0, \nabla c(\mathbf{x}) \rangle \geq 0 \quad \text{for all } \mathbf{x} \in D. \quad (3.2)$$

*Then, there exists a sufficiently small number  $\eta_0 = \eta_0(\mathbf{x}_0, D, \|c\|_{C^1(\overline{D})}) \in (0, 1)$  such that for any  $\eta \in (0, \eta_0]$ , one can choose a sufficiently large number  $\lambda_0 = \lambda_0(D, \eta, c, \mathbf{x}_0) > 1$  and a number  $C = C(D, \eta, c, \mathbf{x}_0)$  such that for all  $z \in C^2(\overline{D_{\eta, \varepsilon}})$  and for all  $\lambda \geq \lambda_0$ , the following pointwise Carleman estimate holds true*

$$W_{\lambda, \eta}^2(\mathbf{x}, t) |c(\mathbf{x}) z_{tt}(\mathbf{x}, t) - \Delta z(\mathbf{x}, t)|^2 \geq C \lambda W_{\lambda, \eta}^2(\mathbf{x}, t) \left( |\nabla z(\mathbf{x}, t)|^2 + |z_t(\mathbf{x}, t)|^2 + \lambda^2 |z(\mathbf{x}, t)|^2 \right) + \operatorname{div}(Z(\mathbf{x}, t)) + Y_t(\mathbf{x}, t) \quad (3.3)$$

for  $(\mathbf{x}, t) \in D_{\eta, \varepsilon}$ . The vector valued function  $Z$  and the function  $Y$  satisfy

$$|Z(\mathbf{x}, t)| \leq C \lambda^3 W_{\lambda, \eta}^2(\mathbf{x}, t) (|\nabla z(\mathbf{x}, t)|^2 + |z_t(\mathbf{x}, t)|^2 + |z(\mathbf{x}, t)|^2) \quad (3.4)$$

and

$$|Y(\mathbf{x}, t)| \leq C \lambda^3 W_{\lambda, \eta}^2(\mathbf{x}, t) \left[ |t| (|\nabla z(\mathbf{x}, t)|^2 + |z_t(\mathbf{x}, t)|^2 + |z(\mathbf{x}, t)|^2) + (|\nabla z(\mathbf{x}, t)| + |z(\mathbf{x}, t)|) |z_t(\mathbf{x}, t)| \right]. \quad (3.5)$$

In particular, if either  $z(\mathbf{x}, 0) = 0$  or  $z_t(\mathbf{x}, 0) = 0$ ,  $Y(\mathbf{x}, 0) = 0$ .

We refer the reader to [26, Lemma 6.1] and [7, Theorem 1.10.2] for the proof of Lemma 3.1. The proof of this Carleman weight function in the case  $c \equiv 1$  is given in [38]. In those publications, the Carleman estimate (3.3) holds true for the function  $z$  in  $C^2(\overline{D_{\eta,\varepsilon}^\pm})$  where

$$D_{\eta,\varepsilon}^\pm = \{(\mathbf{x}, t) \in D \times [-T, T] : |\mathbf{x} - \mathbf{x}_0|^2 - \eta t^2 > \varepsilon\}.$$

Hence, to obtain Lemma 3.1, we need to extend the function  $z$  to  $D_{\eta,\varepsilon}^\pm$ .

Let  $\eta_0$  be the number in Lemma 3.1. Fix  $\varepsilon > 0$  and  $\eta \in (0, \eta_0]$ . Since  $\mathbf{x}_0 \notin \Omega$ , we can choose both of these two numbers sufficiently small; say for e.g.,  $\varepsilon < \frac{P_1^2}{2}$  and  $\eta < \frac{P_1^2}{2T^2}$  where  $P_1 = \min_{\mathbf{x} \in \overline{\Omega}_0} \{|\mathbf{x} - \mathbf{x}_0|\}$ , such that

$$|\mathbf{x} - \mathbf{x}_0|^2 - \eta t^2 > \varepsilon \quad \text{for all } (\mathbf{x}, t) \in \Omega_T. \quad (3.6)$$

**Remark 3.1.** *With the choice of  $\eta$  and  $\varepsilon$  above, the Carleman estimate (3.3) holds true for all  $(\mathbf{x}, t) \in \Omega_T$ .*

We now state the main theorem of the paper. Let  $\delta > 0$  be a noise level. By noise level  $\delta$ , we assume that there is a function  $\mathcal{E}$  in  $H^p(\Omega_T)$  satisfying

$$\|\mathcal{E}\|_{H^p(\Omega_T)} \leq \delta, \quad f|_{\Gamma_T} = f^* + \mathcal{E}|_{\Gamma_T}, \quad g|_{\Gamma_T} = g^* + \partial_\nu \mathcal{E}|_{\Gamma_T} \quad (3.7)$$

where  $f^*$  and  $g^*$  are the noiseless version of the data  $f$  and  $g$  respectively. The true solution to (2.1), with  $f$  and  $g$  replaced by  $f^*$  and  $g^*$  respectively, is denoted by  $u^*$ . That means,  $u^*|_{\Gamma_T} = f^*$  and  $\partial_\nu u^*|_{\Gamma_T} = g^*$ .

**Theorem 3.1** (The convergence of  $\{u_n\}_{n \geq 0}$  to  $u^*$  as the noise tends to 0). *Assume that  $\|F\|_{C^1}$  is a finite number and that the function  $c$  satisfies (3.2). Fix  $\varepsilon \in (0, 1)$  and let  $\eta \in (0, \eta_0]$  be such that (3.6) holds true. Fix  $\gamma \in (0, 1)$ . Then, there exist  $\lambda_0 > 1$  depending only on  $D$ ,  $\eta$ ,  $c$ ,  $\mathbf{x}_0$ ,  $\varepsilon$  and  $\epsilon$  such that for all  $\lambda > \lambda_0$ , we have*

$$\|u_{n+1} - u^*\|_{H_{\lambda,\eta}^1(\Omega_T)}^2 \leq \theta^{n+1} \|u_0 - u^*\|_{H_{\lambda,\eta}^1(\Omega_T)}^2 + C(\delta^{2-2\gamma} + \epsilon \|u^*\|_{H_{\lambda,0}^p(\Omega_T)}^2) \quad (3.8)$$

provided that  $\delta < e^{-\lambda P_2^2/\gamma}$  where  $P_2 = \max_{\mathbf{x} \in \overline{\Omega}} |\mathbf{x} - \mathbf{x}_0|$ . Here,  $C$  is a positive number depending only on  $\Omega$ ,  $D$ ,  $c$ ,  $\mathbf{x}_0$  and  $T$  and  $\theta = C/\lambda \in (0, 1)$ .

**Corollary 3.1.** *By the trace theory, it follows from (3.8) that for all  $n \geq 0$ ,*

$$\|p_{n+1} - p^*\|_{L_\lambda^2(\Omega)}^2 \leq C_1 \theta^{n+1} \|u_0 - u^*\|_{H_{\lambda,\eta}^1(\Omega_T)}^2 + C_2 (\delta^{2-2\gamma} + \epsilon \|u^*\|_{H^p(\Omega_T)}^2) \quad (3.9)$$

where  $C_1$  and  $C_2$  are two positive numbers depending only on  $\Omega$ ,  $D$ ,  $c$ ,  $\mathbf{x}_0$  and  $T$ . In (3.9),  $p_{n+1}(\mathbf{x}) = u_{n+1}(\mathbf{x}, 0)$ ,  $p^*$  is the true source function, and

$$\|p_{n+1} - p^*\|_{L_\lambda^2(\Omega)} = \left[ \int_{\Omega} e^{2\lambda|\mathbf{x}-\mathbf{x}_0|^2} |p_{n+1} - p^*|^2 d\mathbf{x} \right]^{\frac{1}{2}}.$$

In practice, the condition that  $\|F\|_{C^1(\overline{\Omega} \times \mathbb{R} \times \mathbb{R}^d)} < \infty$  might not hold true. In this case, we need to know in advance a number  $M$  such that the true solution  $u^*$  to (2.1) belongs to the ball  $B_M = \{v \in H^p(\Omega_T) : \|v\|_{H^p(\Omega_T)} < M\}$ . This requirement does not weaken our result since  $M$  can be arbitrarily large. In order to compute  $u^*$ , we proceed as follows. Due to the Sobolev embedding

theorem,  $\|u^*\|_{C^1(\bar{\Omega}_T)} < C_3M$  for some constant  $C_3$ . Let  $\chi : \bar{\Omega} \times [0, \infty) \times \mathbb{R} \times \mathbb{R} \times \mathbb{R}^d \rightarrow \mathbb{R}$  be a function in the class  $C^1$  and satisfy

$$\chi(\mathbf{x}, t, s_1, s_2, \mathbf{p}) = \begin{cases} 1 & (s_1^2 + s^2 + |\mathbf{p}|^2)^{1/2} \leq C_3M, \\ \in (0, 1) & C_3M < (s_1^2 + s^2 + |\mathbf{p}|^2)^{1/2} < 2C_3M, \\ 0 & (s_1^2 + s^2 + |\mathbf{p}|^2)^{1/2} \geq 2C_3M. \end{cases}$$

Then, it is obvious that  $u^*$  solves

$$\begin{cases} c(\mathbf{x})u_{tt}(\mathbf{x}, t) = \Delta u(\mathbf{x}, t) + \bar{\mathcal{F}}u(\mathbf{x}, t) & (\mathbf{x}, t) \in \Omega_T, \\ u(\mathbf{x}, t) = f(\mathbf{x}, t) & (\mathbf{x}, t) \in \Gamma_T, \\ \partial_\nu u(\mathbf{x}, t) = g(\mathbf{x}, t) & (\mathbf{x}, t) \in \Gamma_T, \\ u_t(\mathbf{x}, 0) = 0 & \mathbf{x} \in \Omega \end{cases} \quad (3.10)$$

where

$$\bar{\mathcal{F}}u = \chi(\mathbf{x}, t, u, u_t, \nabla u)F(\mathbf{x}, t, u, u_t, \nabla u).$$

We now compute  $u^*$  by solving (3.10) using Algorithm 1 and Theorem 3.1 for  $\bar{\mathcal{F}}$ .

**Remark 3.2.** *The auxiliary step above and the requirement about the knowledge of the number  $M$  is only for the theoretical purpose. In our computations in Section 4, we obtain satisfactory numerical results by applying Algorithm 1 directly on (2.1) rather than (3.10). Although the condition  $\|F\|_{C^1(\bar{\Omega} \times [0, T] \times \mathbb{R} \times \mathbb{R} \times \mathbb{R}^d)} < \infty$  does not satisfy, we do not experience any difficulty.*

We present the proof of this theorem in the next subsection. The proof is motivated by [5, 6, 39].

### 3.2 The proof of Theorem 3.1

Throughout the proof,  $C$  is a generic constant depending only on  $\Omega$ ,  $D$ ,  $c$ ,  $\mathbf{x}_0$ ,  $T$ , and  $\|F\|_{C^1}$ . In the proof, we use the Carleman weighted Sobolev norms  $\|\cdot\|_{H_{\lambda, \eta}^s(\Omega_T)}$  defined in Definition 2.1 with some different values of  $s$ ,  $\lambda$  and  $\eta$ . We split the proof into several steps.

**Step 1.** Define

$$H_0 = \{u \in H^p(\Omega_T) : u_t|_{\Omega \times \{0\}} = 0, u|_{\Gamma_T} = 0, \text{ and } \partial_\nu u|_{\Gamma_T} = 0\}.$$

Fix  $n > 0$ . Since  $u_{n+1}$  is the minimizer of  $J_n$ , defined in (2.4), on  $H$ , by the variational principle, we have for all  $h \in H_0$

$$\begin{aligned} \int_{\Omega_T} W_{\lambda, \eta}^2(\mathbf{x}, t) (c(\mathbf{x})(u_{n+1})_{tt} - \Delta u_{n+1} - \mathcal{F}(u_n)) (c(\mathbf{x})h_{tt} - \Delta h) d\mathbf{x}dt \\ + \epsilon \langle u_{n+1}, h \rangle_{H_{\lambda, 0}^p(\Omega_T)} = 0. \end{aligned} \quad (3.11)$$

On the other hand, since  $u^*$  is the true solution to (2.1), for all  $h \in H_0$ , we have

$$\begin{aligned} \int_{\Omega_T} W_{\lambda, \eta}^2(\mathbf{x}, t) (c(\mathbf{x})u_{tt}^* - \Delta u^* - \mathcal{F}(u^*)) (c(\mathbf{x})h_{tt} - \Delta h) d\mathbf{x}dt + \epsilon \langle u^*, h \rangle_{H_{\lambda, 0}^p(\Omega_T)} \\ = \epsilon \langle u^*, h \rangle_{H_{\lambda, 0}^p(\Omega_T)}. \end{aligned} \quad (3.12)$$

Combining (3.11) and (3.12), for all  $h \in H_0$ , we have

$$\begin{aligned} \int_{\Omega_T} W_{\lambda,\eta}^2(\mathbf{x}, t) (c(\mathbf{x})(u_{n+1} - u^*)_{tt} - \Delta(u_{n+1} - u^*) - (\mathcal{F}(u_n) - \mathcal{F}(u^*))) (c(\mathbf{x})h_{tt} - \Delta h) d\mathbf{x}dt \\ + \epsilon \langle u_{n+1} - u^*, h \rangle_{H_{\lambda,0}^p(\Omega_T)} = -\epsilon \langle u^*, h \rangle_{H_{\lambda,0}^p(\Omega_T)}. \end{aligned} \quad (3.13)$$

Due to (3.7), the function

$$z = u_{n+1} - u^* - \mathcal{E} \quad (3.14)$$

is in  $H_0$ . Using this test function  $h = z$  for the identity (3.13), we have

$$\begin{aligned} \int_{\Omega_T} W_{\lambda,\eta}^2(\mathbf{x}, t) (c(\mathbf{x})(z + \mathcal{E})_{tt} - \Delta(z + \mathcal{E}) - (\mathcal{F}(u_n) - \mathcal{F}(u^*))) \\ (c(\mathbf{x})z_{tt} - \Delta z) d\mathbf{x}dt + \epsilon \langle z + \mathcal{E}, z \rangle_{H_{\lambda,0}^p(\Omega_T)} = -\epsilon \langle u^*, z \rangle_{H_{\lambda,0}^p(\Omega_T)}. \end{aligned}$$

Thus,

$$\begin{aligned} \int_{\Omega_T} W_{\lambda,\eta}^2(\mathbf{x}, t) |c(\mathbf{x})z_{tt} - \Delta z|^2 d\mathbf{x}dt + \epsilon \|z\|_{H_{\lambda,0}^p(\Omega_T)}^2 \\ = \int_{\Omega_T} W_{\lambda,\eta}^2(\mathbf{x}, t) (\mathcal{F}(u_n) - \mathcal{F}(u^*)) (c(\mathbf{x})z_{tt} - \Delta z) d\mathbf{x}dt \\ - \int_{\Omega_T} W_{\lambda,\eta}^2(\mathbf{x}, t) (c(\mathbf{x})\mathcal{E}_{tt} - \Delta \mathcal{E}) (c(\mathbf{x})z_{tt} - \Delta z) - \epsilon \langle u^*, z \rangle_{H_{\lambda,0}^p(\Omega_T)}. \end{aligned} \quad (3.15)$$

Using the inequality  $|ab| \leq 4a^2 + b^2/16$ , we deduce from (3.15) that

$$\begin{aligned} \int_{\Omega_T} W_{\lambda,\eta}^2(\mathbf{x}, t) |c(\mathbf{x})z_{tt} - \Delta z|^2 d\mathbf{x}dt + \epsilon \|z\|_{H_{\lambda,0}^p(\Omega_T)}^2 \leq C \left[ \int_{\Omega_T} W_{\lambda,\eta}^2(\mathbf{x}, t) |\mathcal{F}(u_n) - \mathcal{F}(u^*)|^2 d\mathbf{x}dt \right. \\ \left. + \int_{\Omega_T} W_{\lambda,\eta}^2(\mathbf{x}, t) |c(\mathbf{x})\mathcal{E}_{tt} - \Delta \mathcal{E}|^2 d\mathbf{x}dt + \epsilon \|u^*\|_{H_{\lambda,0}^p(\Omega_T)}^2 \right]. \end{aligned} \quad (3.16)$$

Since  $\|F\|_{C^1(\bar{\Omega} \times \mathbb{R} \times \mathbb{R}^d)} < \infty$ , we can find a constant  $C$  such that

$$|\mathcal{F}(u_n) - \mathcal{F}(u^*)|^2 \leq C[|u_n - u^*|^2 + |(u_n - u^*)_t|^2 + |\nabla(u_n - u^*)|^2] \quad \text{in } \Omega_T.$$

Using this and (3.16), we have

$$\begin{aligned} \int_{\Omega_T} W_{\lambda,\eta}^2(\mathbf{x}, t) |c(\mathbf{x})z_{tt} - \Delta z|^2 d\mathbf{x}dt + \epsilon \|z\|_{H_{\lambda,0}^p(\Omega_T)}^2 \\ \leq C \left[ \int_{\Omega_T} W_{\lambda,\eta}^2(\mathbf{x}, t) (|u_n - u^*|^2 + |(u_n - u^*)_t|^2 + |\nabla(u_n - u^*)|^2) d\mathbf{x}dt \right. \\ \left. + \int_{\Omega_T} W_{\lambda,\eta}^2(\mathbf{x}, t) |c(\mathbf{x})\mathcal{E}_{tt} - \Delta \mathcal{E}|^2 d\mathbf{x}dt + \epsilon \|u^*\|_{H_{\lambda,0}^p(\Omega_T)}^2 \right]. \end{aligned} \quad (3.17)$$

**Step 2.** Due to Remark 3.1, the Carleman estimate (3.3) holds true for the function  $z$  in the whole set  $\Omega_T$ . Integrating (3.3) on  $\Omega_T$ , we have

$$\begin{aligned} & \int_{\Omega_T} W_{\lambda,\eta}^2(\mathbf{x}, t) |c(\mathbf{x}) z_{tt}(\mathbf{x}, t) - \Delta z(\mathbf{x}, t)|^2 dt d\mathbf{x} \\ & \geq C\lambda \int_{\Omega_T} W_{\lambda,\eta}^2(\mathbf{x}, t) \left( |\nabla z(\mathbf{x}, t)|^2 + |z_t(\mathbf{x}, t)|^2 + \lambda^2 |z(\mathbf{x}, t)|^2 \right) dt d\mathbf{x} \\ & \quad + \int_{\Omega_T} \operatorname{div}(Z(\mathbf{x}, t)) dt d\mathbf{x} + \int_{\Omega_T} Y_t(\mathbf{x}, t) dt d\mathbf{x}. \end{aligned} \quad (3.18)$$

Since  $z \in H_0$ ,  $Z(\mathbf{x}, t) = 0$  for all  $\mathbf{x} \in \partial\Omega$ . By the divergence theorem, we have

$$\int_{\Omega_T} \operatorname{div}(Z(\mathbf{x}, t)) dt d\mathbf{x} = 0. \quad (3.19)$$

Using the Fundamental theorem of Calculus, we have

$$\int_{\Omega_T} Y_t(\mathbf{x}, t) dt d\mathbf{x} = \int_{\Omega} \int_0^T Y_t(\mathbf{x}, t) dt d\mathbf{x} = \int_{\Omega} [Y(\mathbf{x}, T) - Y(\mathbf{x}, 0)] d\mathbf{x}. \quad (3.20)$$

Since  $z_t(\mathbf{x}, 0) = 0$  for all  $\mathbf{x} \in \Omega$ , we have  $Y(\mathbf{x}, 0) = 0$ . Using (3.5), we deduce from (3.20) that

$$\left| \int_{\Omega_T} Y_t(\mathbf{x}, t) dt d\mathbf{x} \right| \leq C\lambda^3 \int_{\Omega} W_{\lambda,\eta}^2(\mathbf{x}, T) (|\nabla z(\mathbf{x}, T)|^2 + |z_t(\mathbf{x}, T)|^2 + |z(\mathbf{x}, T)|^2) d\mathbf{x}. \quad (3.21)$$

It follows from (3.18) and (3.21) that

$$\begin{aligned} & \int_{\Omega_T} W_{\lambda,\eta}^2(\mathbf{x}, t) |c(\mathbf{x}) z_{tt}(\mathbf{x}, t) - \Delta z(\mathbf{x}, t)|^2 dt d\mathbf{x} \\ & \geq C\lambda \int_{\Omega_T} W_{\lambda,\eta}^2(\mathbf{x}, t) \left( |\nabla z(\mathbf{x}, t)|^2 + |z_t(\mathbf{x}, t)|^2 + \lambda^2 |z(\mathbf{x}, t)|^2 \right) dt d\mathbf{x} \\ & \quad - C\lambda^3 \int_{\Omega} W_{\lambda,\eta}^2(\mathbf{x}, T) (|\nabla z(\mathbf{x}, T)|^2 + |z_t(\mathbf{x}, T)|^2 + |z(\mathbf{x}, T)|^2) d\mathbf{x}. \end{aligned} \quad (3.22)$$

Using the trace theory on  $H^p(\Omega_T) \hookrightarrow H^1(\Omega \times \{t = T\})$ , we can find a constant  $C_1$  such that

$$\begin{aligned} \lambda^3 e^{-\lambda\eta T^2} \|z\|_{H_{\lambda,0}^p(\Omega_T)}^2 &= \lambda^3 e^{-\lambda\eta T^2} \int_{\Omega_T} \sum_{|\alpha|=0}^p e^{2\lambda|\mathbf{x}-\mathbf{x}_0|^2} |\partial_{\alpha} z|^2 dt d\mathbf{x} \\ &\geq C_1 \lambda^3 \int_{\Omega} W_{\lambda,\eta}^2(\mathbf{x}, T) \left( |\nabla z(\mathbf{x}, T)|^2 + |z_t(\mathbf{x}, T)|^2 + |z(\mathbf{x}, T)|^2 \right) d\mathbf{x} \end{aligned} \quad (3.23)$$

Combining (3.22) and (3.23) gives

$$\begin{aligned} & \int_{\Omega_T} W_{\lambda,\eta}^2(\mathbf{x}, t) |c(\mathbf{x}) z_{tt}(\mathbf{x}, t) - \Delta z(\mathbf{x}, t)|^2 dt d\mathbf{x} + \varepsilon \|z\|_{H_{\lambda,0}^p(\Omega_T)}^2 \\ & \geq C\lambda \int_{\Omega_T} W_{\lambda,\eta}^2(\mathbf{x}, t) \left( |\nabla z(\mathbf{x}, t)|^2 + |z_t(\mathbf{x}, t)|^2 + \lambda^2 |z(\mathbf{x}, t)|^2 \right) dt d\mathbf{x} \\ & \quad + \varepsilon \|z\|_{H_{\lambda,0}^p(\Omega_T)}^2 - C\lambda^3 e^{-\lambda\eta T^2} \|z\|_{H_{\lambda,0}^p(\Omega_T)}^2. \end{aligned} \quad (3.24)$$

**Step 3.** It follows from (3.17) and (3.24) that

$$\begin{aligned}
& C\lambda \int_{\Omega_T} W_{\lambda,\eta}^2(\mathbf{x}, t) \left( |\nabla z(\mathbf{x}, t)|^2 + |z_t(\mathbf{x}, t)|^2 + \lambda^2 |z(\mathbf{x}, t)|^2 \right) dt d\mathbf{x} + \epsilon \|z\|_{H_{\lambda,0}^p(\Omega_T)}^2 \\
& - C\lambda^3 e^{-\lambda\eta T^2} \|z\|_{H_{\lambda,0}^p(\Omega_T)}^2 \leq \int_{\Omega_T} W_{\lambda,\eta}^2(\mathbf{x}, t) (|u_n - u^*|^2 + |(u_n - u^*)_t|^2 + |\nabla(u_n - u^*)|^2) d\mathbf{x} dt \\
& + \int_{\Omega_T} W_{\lambda,\eta}^2(\mathbf{x}, t) |c(\mathbf{x}) \mathcal{E}_{tt} - \Delta \mathcal{E}|^2 d\mathbf{x} dt + \epsilon \|u^*\|_{H_{\lambda,0}^p(\Omega_T)}^2. \quad (3.25)
\end{aligned}$$

Recall from (3.14) that  $z = u_{n+1} - u^* - \mathcal{E}$  and the inequality  $(a + b)^2 \geq \frac{1}{2}a^2 - b^2$ . Fix  $\lambda \geq \frac{\ln C - \ln \epsilon}{\eta T^2}$  such that  $C\lambda^3 e^{-\lambda\eta T^2} < \epsilon$ . It follows from (3.25) that

$$\lambda \|u_{n+1} - u^*\|_{H_{\lambda,\eta}^1(\Omega_T)}^2 \leq C \|u_n - u^*\|_{H_{\lambda,\eta}^1(\Omega_T)}^2 + C\lambda \|\mathcal{E}\|_{H_{\lambda,\eta}^p(\Omega_T)}^2 + \epsilon \|u^*\|_{H_{\lambda,0}^p(\Omega_T)}^2. \quad (3.26)$$

Therefore,

$$\|u_{n+1} - u^*\|_{H_{\lambda,\eta}^1(\Omega_T)}^2 \leq \frac{C}{\lambda} \|u_n - u^*\|_{H_{\lambda,\eta}^1(\Omega_T)}^2 + C \|\mathcal{E}\|_{H_{\lambda,\eta}^p(\Omega_T)}^2 + \frac{\epsilon}{\lambda} \|u^*\|_{H_{\lambda,0}^p(\Omega_T)}^2. \quad (3.27)$$

Since  $\|\mathcal{E}\|_{H^p(\Omega)} < \delta$ ,  $\|\mathcal{E}\|_{H_{\lambda,\eta}^p(\Omega)}^2 \leq e^{2\lambda P_2^2} \delta^2$  where  $P_2 = \max_{\mathbf{x} \in \bar{\Omega}} \{|\mathbf{x} - \mathbf{x}_0|\}$ . For any  $\gamma \in (0, 1)$ . If  $\delta < e^{-\lambda P_2^2/\gamma}$  then it is obvious that  $\|\mathcal{E}\|_{H_{\lambda,\eta}^p(\Omega_T)}^2 < \delta^{2-2\gamma}$ . In this case, it follows from (3.27) that

$$\|u_{n+1} - u^*\|_{H_{\lambda,\eta}^1(\Omega_T)}^2 \leq \theta \|u_n - u^*\|_{H_{\lambda,\eta}^1(\Omega_T)}^2 + C(\delta^{2-2\gamma} + \epsilon \|u^*\|_{H_{\lambda,0}^p(\Omega_T)}^2) \quad (3.28)$$

where  $\theta = C/\lambda \in (0, 1)$ . Applying (3.28) with  $n$  replaced by  $n-1, \dots, 1$ , we obtain (3.8). The proof is complete.

## 4 Numerical study

For simplicity, we numerically solve Problem 1.1 in the 2-dimensional case. We set  $\Omega = (-1, 1)^2$ . To solve the forward problem, we approximate  $\mathbb{R}^2$  by the square  $G = (-R, R)^2$  where  $R > 1$  is a large number. We then employ the explicit scheme to solve (1.1) on  $G$ . In our computation,  $R = 4$ . We set the final time  $T = 2 < 4$ . In this setting, the nonlinear wave generated by an unknown source supported inside  $\Omega$  does not have enough time to propagate to  $\partial G$ . Therefore, the computed wave is the restriction of the solution to (1.1) on  $G \times [0, T]$ . Our implementation is based on the finite difference method, in which the step size in space is  $d_{\mathbf{x}} = 0.03$  and the step size in time is  $d_t = 0.0132$ . These values of step sizes in space and time are chosen such that  $d_t/d_{\mathbf{x}} = 0.44 < 0.5$ . Thus, the computed wave by the explicit scheme is reliable.

In this section, we set the noise level  $\delta = 10\%$ . That means the data we use are given by

$$f(\mathbf{x}, t) = f^*(\mathbf{x}, t)(1 + \delta \text{rand}) \quad \text{and} \quad g(\mathbf{x}, t) = g^*(\mathbf{x}, t)(1 + \delta \text{rand})$$

for all  $(\mathbf{x}, t) \in \Gamma_T$  and rand is the function taking uniformly distributed random number in the range  $[-1, 1]$ . In all of our numerical examples, the stopping number  $n_0$  in Step 2 of Algorithm 1 is set to be 7. It is not necessary to set  $n_0$  as a bigger number. This is because of the fast convergence of the exponential rate  $O(\theta^n)$  as  $n \rightarrow \infty$  for some  $\theta \in (0, 1)$ . See Theorem 3.1 and (3.8).

Implementing Algorithm 1 is straight forward. The most complicated part is Step 3. That is how to minimize a function  $J_n$  defined in (2.4). This step is equivalent to the problem solving a linear equation subject to some boundary and initial constraints by the quasi-reversibility method. We employ the optimization package built-in in MATLAB with the command “lsqin” for this step. The implementation is very similar to the one described in [44, Section 6]. We do not repeat the details of implementation here. Although the norm in the regularization term is  $H_{\lambda,0}^p(\Omega_T)$ , in our computational program, we use a simpler norm  $H_{\lambda,0}^2(\Omega_T)$  to simplify the computational scripts. This change does not effect the satisfactory outputs. The ”artificial” parameters for all tests below are:  $\epsilon = 10^{-14}$ ,  $\lambda = 2.1$  and  $\eta = 0.5$ . These parameters are numerically chosen such that the reconstruction result is satisfactory for test 1. Then, we use these values for all other tests.

Regarding the initial solution  $u_0$ , we have mentioned in Step 1 of Algorithm 1 that  $u_0$  can be any function in  $H$ . That means we can take any function in  $H^p(\Omega_T)$  such that  $u|_{\Gamma_T} = f$ ,  $\partial_\nu u|_{\Gamma_T} = g$  and  $u_t|_{\Omega \times \{t=0\}} = 0$ . A natural way to compute such a function  $u_0$  is to find a function  $u$  satisfying

$$\begin{cases} \Delta u(\mathbf{x}, t) = 0 & (\mathbf{x}, t) \in \Omega_T, \\ u(\mathbf{x}, t) = f & (\mathbf{x}, t) \in \Gamma_T, \\ u(\mathbf{x}, t) = g & (\mathbf{x}, t) \in \Gamma_T, \\ u_t(\mathbf{x}, 0) = 0 & \mathbf{x} \in \Omega. \end{cases} \quad (4.1)$$

We do so by the quasi-reversibility method. That means we set  $u_0$  as the minimizer of

$$\int_{\Omega_T} W_{\lambda,\eta}^2(\mathbf{x}, t) |\Delta u|^2 dt d\mathbf{x} + \epsilon \|u\|_{H_\lambda^2(\Omega_T)}$$

subject to the constraints as in the last three lines of (4.1). Again, we refer the reader to [44, Section 6] for the details in implementation of the quasi-reversibility method using the optimization package of MATLAB.

We show four (4) numerical tests.

**Test 1.** In this test, we set the nonlinearity  $f$  to be

$$f(\mathbf{x}, t, u, u_t, \nabla u) = \sqrt{u^2 + 1} + |\nabla u|$$

and the true source function is

$$p^*(x, y) = \begin{cases} 15e^{\frac{r^2(x,y)}{r^2(x,y)-1}} & \text{if } r(x, y) < 1, \\ 0 & \text{otherwise} \end{cases}$$

where  $r(x, y) = \frac{x^2}{0.5^2} + \frac{y^2}{0.8^2}$ . The support of the true source function  $p^*$  is an ellipse centered at the origin with the  $x$ -radius 0.5 and  $y$ -radius 0.8. The maximum value of  $p^*$  is 15. In this test, the true function  $p^*$  is far away from the background. So, finding an initial guess is impossible. The numerical result of this test is displayed in Figure 1.

It is evident from Figures 1c–1d that we successfully compute the source function without requesting an initial guess. In fact, the initial solution  $p_{init}$  obtained by solving (4.1) by the quasi-reversibility method is almost equal to the zero function. It is far away from the true solution  $p^*$ , see Figure 1b. It follows from Figure 1e that our method converges fast after only 4 iterations. This observation is consistent to the conclusion of Theorem 3.1. The  $L^2$ -relative error  $\frac{\|p_{comp} - p^*\|_{L^2(\Omega)}}{\|p^*\|_{L^2(\Omega)}}$  in Test 1 is 5.4%.

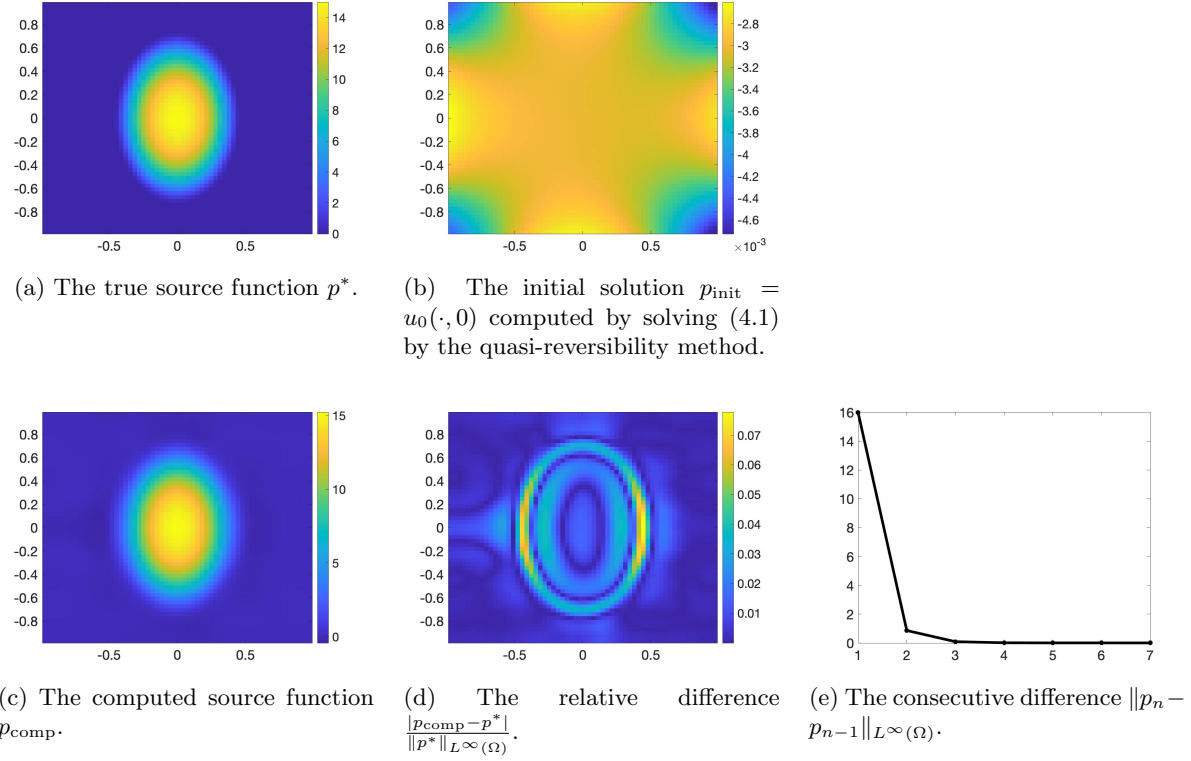


Figure 1: Test 1. The true and computed source functions. The computed source function can be successfully found although the support of the source function is large and the value of this function is 15, which is high. The initial solution  $p_{\text{init}}$  is faraway from  $p^*$ .

**Test 2.** We consider the source function with more complicated structure. The true source function is given by

$$p^*(x, y) = \sin(\pi(x + y)) + \sin((2\pi(x - y))) \quad \text{for all } \mathbf{x} = (x, y) \in \Omega.$$

The nonlinearity in this test is a bounded function

$$f(\mathbf{x}, t, u, u_t, \nabla u) = \min\{e^u + |\nabla u|, 10\}.$$

Although the nonlinearity  $f$  is not in the class  $C^1$  and the geometric structure of the true source function is complicated, one will see that Algorithm 1 is effective, see Figure 2.

As in Test 1, it is evident from Figures 2c–2d that we successfully compute the source function without requesting an initial guess. In fact, the initial solution  $p_{\text{init}}$  obtained by solving (4.1) by the quasi-reversibility method is far away from the true solution  $p^*$ , see Figure 2b. It follows from Figure 2e that our method converges fast after only 5 iterations. This observation is consistent to the conclusion of Theorem 3.1. The  $L^2$ -relative error  $\frac{\|p_{\text{comp}} - p^*\|_{L^2(\Omega)}}{\|p^*\|_{L^2(\Omega)}}$  in Test 1 is 7.07%.

**Test 3.** We test the case when the true source function is not smooth, given by the following piece-wise constant function

$$p^*(x, y) = \begin{cases} 15 & \text{if } \max\left\{\frac{|x-0.4|}{0.15}, \frac{|y|}{0.7}\right\} < 1 \text{ or } (x + 0.4)^2 + y^2 < 0.04, \\ 0 & \text{otherwise.} \end{cases}$$

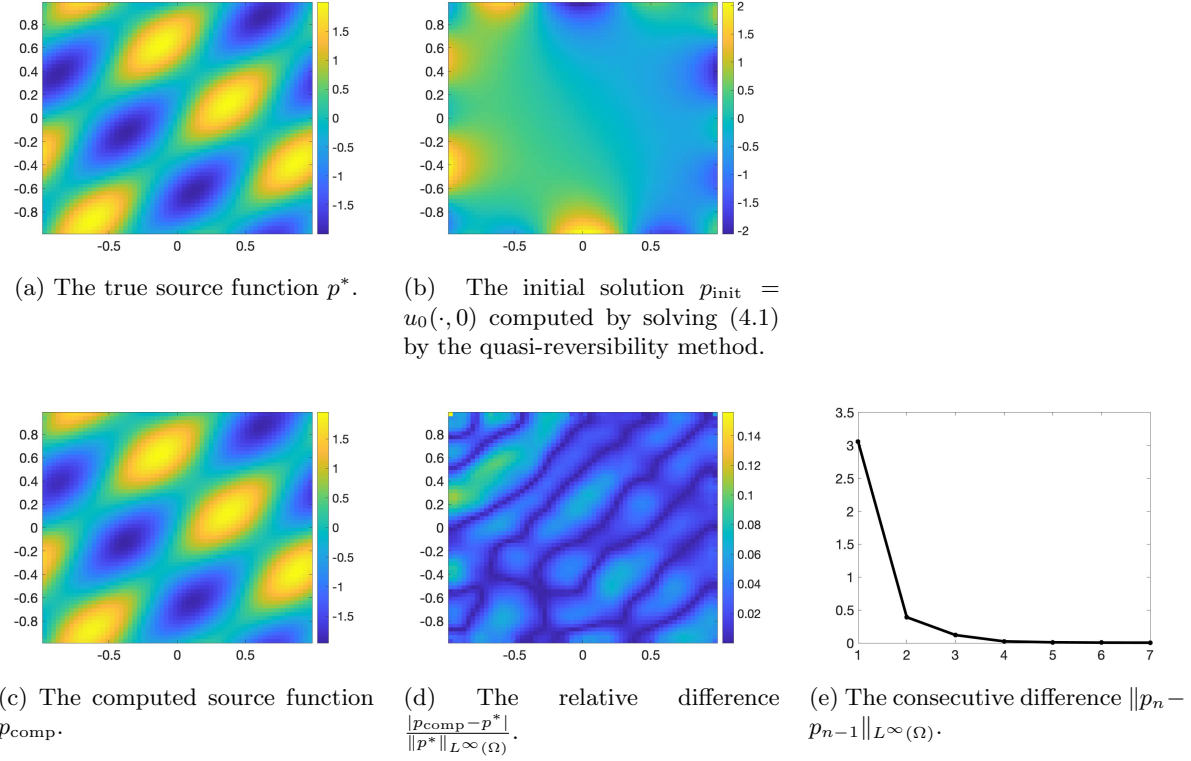


Figure 2: Test 2. The true and computed source functions. The computed source function can be successfully found although the geometry structure of  $p^*$  is complicated and the nonlinearity  $f$  is not in the class  $C^1$ .

The support of  $p^*$  involves a vertical rectangle and a disk. The maximum value of  $p^*$  is 15. Finding an initial guess for this function is impossible. In this test, we use the nonlinearity

$$f(\mathbf{x}, t, u, u_t, \nabla u) = \min\{u^2 + 1, 10\} + |\nabla u|.$$

Like Test 2, the nonlinearity in this test is not in the class  $C^1$  but unlike Test 2,  $f$  is unbounded. The computed solution to Problem 1.1 of Test 3 is displayed in Figure 3.

The numerical result is satisfactory. One can see that we can effectively reconstruct both rectangular and circular “inclusions”. The maximum value of  $p_{\text{comp}}$  is 15.8 (relative error is 5.3%). Unlike the case when  $p^*$  is smooth, the  $L^2$  relative error in this test is high 34.5%. However, one can see from Figure 3d that the large error occurs significantly on the borders of the inclusions while the error is small almost everywhere. Like in Test 1 and Test 2, the convergence rate of Algorithm 1 is fast. One can see from Figure 3e that we can obtain the computed source function with only 4 iterations.

**Test 4.** We now consider a more complicated case when the true source function has large contrast and its circular support has a rectangular void. The function  $p^*$  is given by

$$p^*(x, y) = \begin{cases} 25 & \text{if } x^2 + y^2 < 0.65^2 \text{ and } \max\{|x|, |y|\} > 0.35, \\ 0 & \text{otherwise.} \end{cases}$$

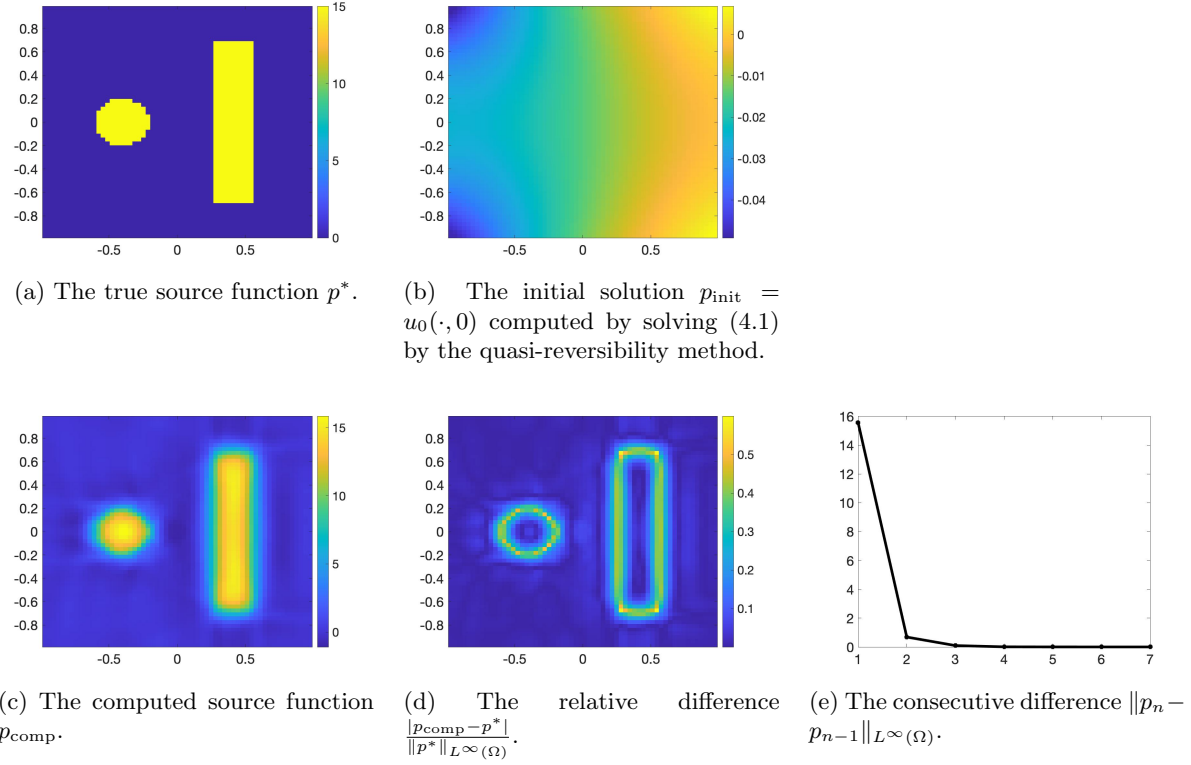


Figure 3: Test 3. The true and computed source functions. The computed source function can be successfully found although  $p^*$  is far away from the background zeros function and the nonlinearity  $f$  is not in the class  $C^1$  and not bounded.

The nonlinearity in this test is set to be

$$f(\mathbf{x}, t, u, u_t, \nabla u) = \min\{e^u, 100\} + |\nabla u|.$$

The nonlinearity in this test is not bounded nor in the class  $C^1$ . The numerical result for this test is in Figure 4.

Although the true source function  $p^*$  and the nonlinearity in this test is complicated, the obtained numerical result is out of expectation. One can see that we can effectively reconstruct the shape of the support of the source function. The maximum value of  $p_{\text{comp}}$  is 25.087 (relative error is 0.4%). Unlike the case when  $p^*$  is smooth, the  $L^2$  relative error in this test is high 36.0%. However, one can see from Figure 4d that the large error occurs significantly on the borders of the support of  $p^*$  while the error is small almost everywhere. Like in all tests above, the convergence rate of Algorithm 1 is fast. One can see from Figure 4e that we can obtain the computed source function with only 7 iterations.

## 5 Concluding remarks

We have solve an inverse problem that is to reconstruct the initial condition of nonlinear hyperbolic equation. Although this problem is nonlinear, we solve it globally. That means we do not

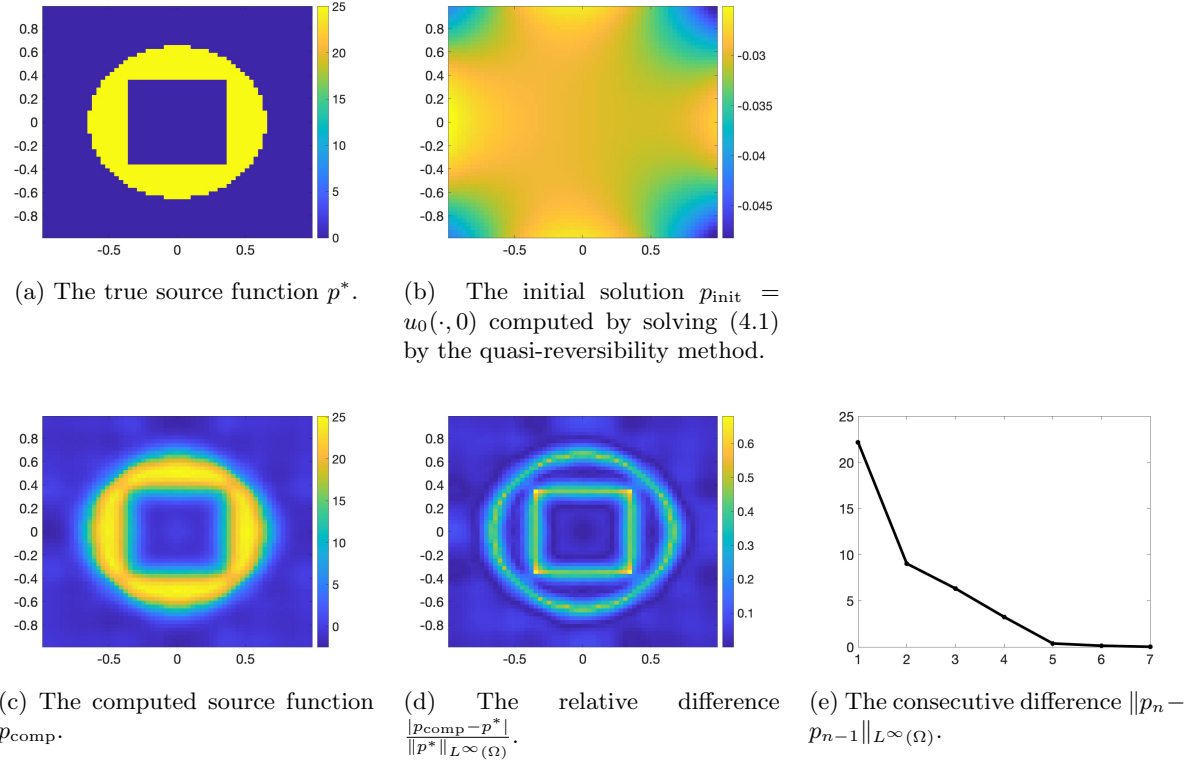


Figure 4: Test 4. The true and computed source functions. The computed source function can be successfully found although  $p^*$  is far away from the background zeros function and the nonlinearity  $f$  is not in the class  $C^1$  and not bounded.

require a good initial guess. We first define an operator  $\Phi$  such that the true solution to the inverse problem is the fixed point of  $\Phi$ . We construct a recursive sequence  $\{u_n\}_{n \geq 0}$  whose initial term  $u_0$  can be taken arbitrary and the  $n^{\text{th}}$  term  $u_n = \Phi(u_{n-1})$ . We next apply a Carleman estimate to prove the convergence of this sequence. The convergence is of the exponential rate. Moreover, we have proved that the stability of our method with respect to noise is of the Hölder type. Numerical results are satisfactory.

## Acknowledgement

This work was supported by US Army Research Laboratory and US Army Research Office grant W911NF-19-1-0044.

## References

- [1] S. Acosta and B. Palacios. Thermoacoustic tomography for an integro-differential wave equation modeling attenuation. *J. Differential Equations*, 5:1984–2010, 2018.
- [2] H. Ammari, E. Bretin, J. Garnier, and V. Wahab. Time reversal in attenuating acoustic media. *Contemp. Math.*, 548:151–163, 2011.

- [3] H. Ammari, E. Bretin, E. Jugnon, and V. Wahab. Photoacoustic imaging for attenuating acoustic media. In H. Ammari, editor, *Mathematical Modeling in Biomedical Imaging II*, pages 57–84. Springer, 2012.
- [4] A. B. Bakushinskii, M. V. Klibanov, and N. A. Koshev. Carleman weight functions for a globally convergent numerical method for ill-posed Cauchy problems for some quasilinear PDEs. *Nonlinear Anal. Real World Appl.*, 34:201–224, 2017.
- [5] L. Baudouin, M. de Buhan, and S. Ervedoza. Convergent algorithm based on Carleman estimates for the recovery of a potential in the wave equation. *SIAM J. Numer. Anal.*, 55:1578–1613, 2017.
- [6] L. Baudouin, M. de Buhan, S. Ervedoza, and A. Osses. Carleman-based reconstruction algorithm for the waves. *SIAM Journal on Numerical Analysis*, 59(2):998–1039, 2021.
- [7] L. Beilina and M. V. Klibanov. *Approximate Global Convergence and Adaptivity for Coefficient Inverse Problems*. Springer, New York, 2012.
- [8] H. Brézis. *Functional Analysis, Sobolev Spaces and Partial Differential Equations*. Springer, New York, 2011.
- [9] P. Burgholzer, H. Grün, M. Haltmeier, R. Nuster, and G. Paltauf. Compensation of acoustic attenuation for high-resolution photoacoustic imaging with line detectors. *Proc. SPIE*, 6437:643724, 2007.
- [10] C. Clason and M. V. Klibanov. The quasi-reversibility method for thermoacoustic tomography in a heterogeneous medium. *SIAM J. Sci. Comput.*, 30:1–23, 2007.
- [11] N. Do and L. Kunyansky. Theoretically exact photoacoustic reconstruction from spatially and temporally reduced data. *Inverse Problems*, 34(9):094004, 2018.
- [12] L. C. Evans. *Partial Differential Equations*. Graduate Studies in Mathematics, Volume 19. Amer. Math. Soc., 2010.
- [13] M. Haltmeier. Inversion of circular means and the wave equation on convex planar domains. *Comput. Math. Appl.*, 65:1025–1036, 2013.
- [14] M. Haltmeier and L. V. Nguyen. Reconstruction algorithms for photoacoustic tomography in heterogeneous damping media. *Journal of Mathematical Imaging and Vision*, 61:1007–1021, 2019.
- [15] M. Hanke, A. Neubauer, and O. Scherzer. A convergence analysis of the landweber iteration for nonlinear ill-posed problems. *Numer. Math.*, 72:21–37, 1995.
- [16] A. Homan. Multi-wave imaging in attenuating media. *Inverse Probl. Imaging*, 7:1235–1250, 2013.
- [17] Y. Hristova. Time reversal in thermoacoustic tomography—an error estimate. *Inverse Problems*, 25:055008, 2009.

- [18] Y. Hristova, P. Kuchment, and L. V. Nguyen. Reconstruction and time reversal in thermoacoustic tomography in acoustically homogeneous and inhomogeneous media. *Inverse Problems*, 24:055006, 2008.
- [19] C. Huang, K. Wang, L. Nie, L. V. Wang, and M. A. Anastasio. Full-wave iterative image reconstruction in photoacoustic tomography with acoustically inhomogeneous media. *IEEE Trans. Med. Imaging*, 32:1097–1110, 2013.
- [20] V. Katsnelson and L. V. Nguyen. On the convergence of time reversal method for thermoacoustic tomography in elastic media. *Applied Mathematics Letters*, 77:79–86, 2018.
- [21] V. A. Khoa, G. W. Bidney, M. V. Klibanov, L. H. Nguyen, L. Nguyen, A. Sullivan, and V. N. Astratov. Convexification and experimental data for a 3D inverse scattering problem with the moving point source. *Inverse Problems*, 36:085007, 2020.
- [22] V. A. Khoa, G. W. Bidney, M. V. Klibanov, L. H. Nguyen, L. Nguyen, A. Sullivan, and V. N. Astratov. An inverse problem of a simultaneous reconstruction of the dielectric constant and conductivity from experimental backscattering data. *Inverse Problems in Science and Engineering*, 29(5):712–735, 2021.
- [23] V. A. Khoa, M. V. Klibanov, and L. H. Nguyen. Convexification for a 3D inverse scattering problem with the moving point source. *SIAM J. Imaging Sci.*, 13(2):871–904, 2020.
- [24] M. V. Klibanov. Global convexity in a three-dimensional inverse acoustic problem. *SIAM J. Math. Anal.*, 28:1371–1388, 1997.
- [25] M. V. Klibanov. Global convexity in diffusion tomography. *Nonlinear World*, 4:247–265, 1997.
- [26] M. V. Klibanov. Carleman estimates for the regularization of ill-posed Cauchy problems. *Applied Numerical Mathematics*, 94:46–74, 2015.
- [27] M. V. Klibanov. Carleman weight functions for solving ill-posed Cauchy problems for quasi-linear PDEs. *Inverse Problems*, 31:125007, 2015.
- [28] M. V. Klibanov and O. V. Ioussoupova. Uniform strict convexity of a cost functional for three-dimensional inverse scattering problem. *SIAM J. Math. Anal.*, 26:147–179, 1995.
- [29] M. V. Klibanov and A. E. Kolesov. Convexification of a 3-D coefficient inverse scattering problem. *Computers and Mathematics with Applications*, 77:1681–1702, 2019.
- [30] M. V. Klibanov, T. T. Le, L. H. Nguyen, A. Sullivan, and L. Nguyen. Convexification-based globally convergent numerical method for a 1D coefficient inverse problem with experimental data. *preprint, arXiv:2104.11392*, 2021.
- [31] M. V. Klibanov, J. Li, and W. Zhang. Convexification of electrical impedance tomography with restricted Dirichlet-to-Neumann map data. *Inverse Problems*, 35:035005, 2019.
- [32] M. V. Klibanov, Z. Li, and W. Zhang. Convexification for the inversion of a time dependent wave front in a heterogeneous medium. *SIAM J. Appl. Math.*, 79:1722–1747, 2019.
- [33] R. Kowar. On time reversal in photoacoustic tomography for tissue similar to water. *SIAM J. Imaging Sci.*, 7:509–527, 2014.

- [34] R. Kowar and O. Scherzer. Photoacoustic imaging taking into account attenuation. In H. Ammari, editor, *Mathematics and Algorithms in Tomography II, Lecture Notes in Mathematics*, pages 85–130. Springer, 2012.
- [35] R. A. Kruger, P. Liu, Y. R. Fang, and C. R. Appledorn. Photoacoustic ultrasound (PAUS)–reconstruction tomography. *Med. Phys.*, 22:1605, 1995.
- [36] R. A. Kruger, D. R. Reinecke, and G. A. Kruger. Thermoacoustic computed tomography: technical considerations. *Med. Phys.*, 26:1832, 1999.
- [37] R. Lattès and J. L. Lions. *The Method of Quasireversibility: Applications to Partial Differential Equations*. Elsevier, New York, 1969.
- [38] M. M. Lavrent’ev, V. G. Romanov, and S. P. Shishat’skii. *Ill-Posed Problems of Mathematical Physics and Analysis*. Translations of Mathematical Monographs. AMS, Providence: RI, 1986.
- [39] T. T. Le and L. H. Nguyen. A convergent numerical method to recover the initial condition of nonlinear parabolic equations from lateral Cauchy data. *Journal of Inverse and Ill-posed Problems*, DOI: <https://doi.org/10.1515/jiip-2020-0028>, 2020.
- [40] T. T. Le and L. H. Nguyen. The gradient descent method for the convexification to solve boundary value problems of quasi-linear PDEs and a coefficient inverse problem. *preprint arXiv:2103.04159*, 2021.
- [41] T. T. Le, L. H. Nguyen, T-P. Nguyen, and W. Powell. The quasi-reversibility method to numerically solve an inverse source problem for hyperbolic equations. *Journal of Scientific Computing*, 87:90, 2021.
- [42] A. I. Nachman, J. F. Smith III, and R.C. Waag. An equation for acoustic propagation in inhomogeneous media with relaxation losses. *J. Acoust. Soc. Am.*, 88:1584–1595, 1990.
- [43] F. Natterer. Photo-acoustic inversion in convex domains. *Inverse Probl. Imaging*, 6:315–320, 2012.
- [44] L. H. Nguyen. An inverse space-dependent source problem for hyperbolic equations and the Lipschitz-like convergence of the quasi-reversibility method. *Inverse Problems*, 35:035007, 2019.
- [45] L. V. Nguyen. A family of inversion formulas in thermoacoustic tomography. *Inverse Probl. Imaging*, 3:649–675, 2009.
- [46] A. Oraevsky, S. Jacques, R. Esenaliev, and F. Tittel. Laser-based optoacoustic imaging in biological tissues. *Proc. SPIE*, 2134A:122, 1994.
- [47] G. Paltauf, R. Nuster, M. Haltmeier, and P. Burgholzer. Experimental evaluation of reconstruction algorithms for limited view photoacoustic tomography with line detectors. *Inverse Problems*, 23:S81–S94, 2007.
- [48] G. Paltauf, J. A. Viator, S. A. Prahl, and S. L. Jacques. Iterative reconstruction algorithm for optoacoustic imaging. *J. Opt. Soc. Am.*, 112:1536–1544, 2002.
- [49] P. Stefanov and G. Uhlmann. Thermoacoustic tomography with variable sound speed. *Inverse Problems*, 25:075011, 2009.

- [50] P. Stefanov and G. Uhlmann. Thermoacoustic tomography arising in brain imaging. *Inverse Problems*, 27:045004, 2011.